

Supporting Information

Reactivity of *N*-Boc-3-nitro-7-azaindole: adduct characterization and kinetics of the reactions with carbanions

Tianyu Zhang and Armin R. Ofial*

Department Chemie, Ludwig-Maximilians-Universität München, Butenandtstr. 5-13, 81377 München, Germany,
E-mail: ofial@lmu.de

Data storage system:

Main folder 'analytics':

Subfolders contain raw and evaluated analytics data for the Wheland σ -complexes, which were characterized in d_6 -DMSO solution by high-resolution mass spectrometry (HRMS) and nuclear magnetic resonance (NMR) spectroscopy and by additional UV-Vis spectra in DMSO.

Subfolder 'UV-Vis Wheland adducts':

The files *.xlsx/*.ods contain the time-dependent absorption spectra for mixtures of **11a** with carbanions **12** (Microsoft Office Professional Plus 2016, Microsoft Excel 2016 MSO 16.0).

Subfolder 'HRMS Wheland adducts WA':

The files *.pdf are PDF copies of the HRMS spectra [evaluated data].

The files *.raw contain HRMS raw data that can be opened with the software package FreeStyle 1.8 SP2 QF1 (ThermoFisher Scientific, <https://docs.thermofisher.com/p/desktop-software>).

Subfolder 'NMR Wheland adducts WA':

The files *.mnova contain the acquired one- and two-dimensional NMR spectral data that can be opened with the software package MestReNova (used version: 15.0.0-34764) from Mestrelab Research S. L.

The files *.zip contain the unprocessed (raw) files in various formats as generated by the NMR spectrometers during data acquisition.

Main folder 'kinetics':

Subfolders 'EDA 11a + 12' contain

- *.txt files with absorbance vs. time data [raw data]
- *.exp files used for the k_{obs} determination [evaluated data]
- *.pdf files with results of the k_{obs} determination [evaluated data].

Folder names refer to individual electrophile/nucleophile combinations (as in Tables S2-S8) in this Supporting Information.

Compound labels (that is, **11a** for the electrophile and **12a–12h** for the nucleophiles) are identical to those in this Supporting Information.

Table of Contents

| | |
|---|-----|
| 1. General..... | S3 |
| 2. Kinetic experiments for the determination of the electrophilicity of the EDA 11a | S4 |
| 2.1 Strategy for the electrophilicity determination | S4 |
| 2.2 NMR and HRMS detection of covalent adducts of carbanions and 11a | S7 |
| 2.3 UV-Vis spectra of mixtures of C-nucleophiles (12) with the 11a | S12 |
| 2.4 Kinetics of the reactions of 11a with carbanions (reference nucleophiles 12) | S16 |
| 3. References..... | S23 |

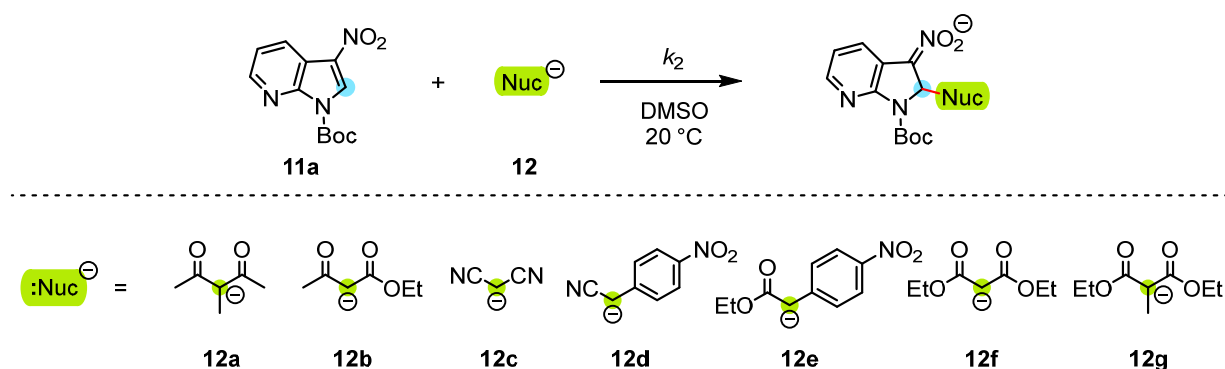
1. General

Analytics

^1H NMR (400 MHz) and $^{13}\text{C}\{^1\text{H}\}$ NMR (101 MHz) spectra were measured on Bruker or Varian NMR spectrometers. The chemical shifts are given in ppm and refer to the solvent residual signal as internal standard (d_6 -DMSO: $\delta_{\text{H}} = 2.50$ ppm, $\delta_{\text{C}} = 39.52$ ppm).^{S1} ^{13}C NMR spectra were measured with proton decoupling. Abbreviations were used for signal multiplicities: s = singlet, d = doublet, t = triplet, q = quartet, m = multiplet, br = broad signal. Signal assignments are based on additional 2D NMR experiments (H,H-COSY, HSQC, HMBC). High resolution mass spectra (HRMS) were obtained from a Thermo Finnigan MAT 95 instrument (EI) or a Thermo Finnigan LTQ FT (ESI).

Materials

Unless otherwise noted, all chemicals, reagents, and solvents for the performed reactions were commercially available. Compound labels follow the same system as in



N-Boc-3-nitro-7-azaindole (= *tert*-Butyl 3-nitro-1*H*-pyrrolo[2,3-*b*]pyridine-1-carboxylate) (**11a**) is a known compound (ref.S2).

C-Nucleophiles 12. To prepare the reference nucleophiles **12**, potassium *tert*-butoxide (1.0 equiv.) was dissolved in a minimal amount of dry ethanol in a flame-dried Schlenk flask under a dry nitrogen atmosphere. Then, the CH acid **12-H** (1.1 equiv.) was added dropwise to the KO^{*t*}Bu solution at 0 °C. The resulting suspension was stirred for 30 min. The reaction mixture was filtered through a Schlenk frit, and the collected solid was washed with dry diethyl ether and *n*-pentane. The solids were dried under vacuum for 2 h to afford **12**. The ^1H NMR spectra of **12** were in accord with those reported in refs. S3.

Kinetics

Reactions of Electrophile 11a with Carbanions (Reference Nucleophiles 12). The rates of all investigated reactions between the electrophilic **11a** and the carbanionic reference nucleophiles **12** were determined photometrically at 20 °C in DMSO. The kinetics were monitored using stopped-flow UV-Vis spectrometers (Applied Photophysics SX.20MV-R). All solutions were prepared by using dry DMSO (ThermoScientific, DMSO 99.7+%, extra dry, over molecular sieve, AcroSeal) and kept under an atmosphere of dry nitrogen. All kinetic measurements were carried out under exclusion of moisture (N_2 atmosphere) in an air-conditioned laboratory. The solutions' temperature during the monitored reactions was kept at $(20.0 \pm 0.1)^\circ\text{C}$ by using a circulating bath thermostat. In all kinetic runs, the concentration of the excessive reactant was at least ten times higher than the concentration of the reference electrophile, resulting in pseudo-first-order kinetics with an exponential increase of the absorption due to the formation of a UV-detectable σ -complex ($\lambda = 377\text{--}390$ nm). Only the kinetics of the reactions of **11a** with the colored carbanion solution of **12d** was recorded by following the decay of the carbanion's absorption in the visible range of the electromagnetic spectrum ($\lambda = 537$ nm). The kinetic measurements for each **11a** + **12** combination were performed with or without added 18-crown-6 ether (18-c-6) and in some cases with additional CH-acid.

2. Kinetic experiments for the determination of the electrophilicity of the EDA **11a**

2.1 Strategy for the electrophilicity determination

In order to evaluate the Mayr electrophilicity E of *tert*-butyl 3-nitro-1*H*-pyrrolo[2,3-*b*]pyridine-1-carboxylate (**11a**), we measured the rate constants of the addition reactions of carbanionic reference nucleophiles **12a–12g** to the electron-deficient arene **11a** (Figure S1).

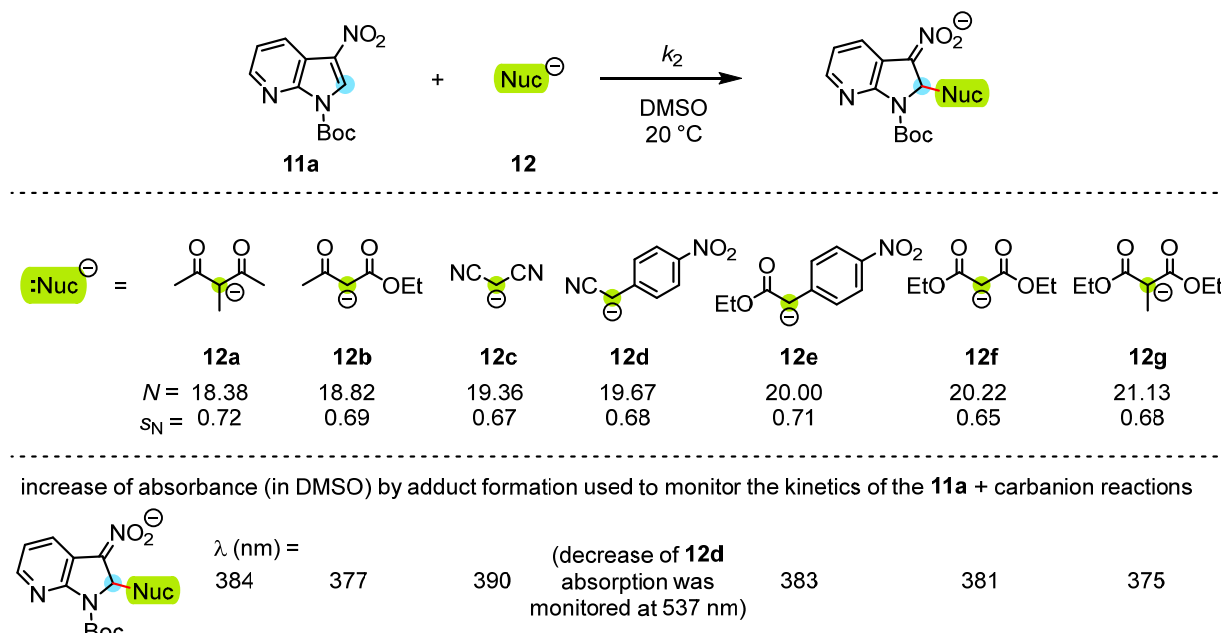


Figure S1: Reference nucleophiles **12** (counterion: K^+) used to characterize the electrophilicity of **11a** (reactivity parameters N and s_N refer to DMSO solution and are from ref. S4).

The carbanions **12a** and **12f** were selected to characterize typical adducts from reactions of carbanions with **11a** by NMR spectroscopic and HRMS analytical methods. In addition, the adduct of **11a** with **12h**, the methylated analog of **12b**, was studied by the same methods (Section 2.2). The HRMS analytics indicated formation of molecular anions for which m/z corresponds to the formation of the anionic adduct. The NMR spectra for adducts of **11a** with **12a** and **12f** indicated the formation of only one product, respectively. The HMBC spectra of these two adduct solutions showed unequivocally C-C bond-formation between the C-2 of the electrophile and the carbanionic center of **12a** and **12f**, respectively. The 3:2 product mixture of the reaction of **12h** with **11a** could potentially be the result of competing O- and C-attack of the ambident nucleophile **12h** at **11a**. However, also in this case, the HMBC spectrum shows that both detected products correspond to C-attack, which generates a mixture of diastereomeric adducts. We, therefore, assumed analogous reactions for all kinetically investigated carbanion combinations with EDA **11a** as depicted in FigureS1, top.

The kinetics of EDA **11a** + **12** reactions (Figure S2a) in DMSO at 20 °C were monitored photometrically by stopped-flow UV-VIS spectroscopy. In general, we followed the increase of absorption caused by formation of the σ -complex from **11a** and the carbanionic nucleophiles **12** (Figure S2b). Thus, the kinetics of **11a** + **12a–12c** and **11a** + **12e–12g** reactions were monitored at wavelengths in the range of $\lambda_{\text{max}} = 375\text{--}390$ nm (see details in Section 2.3). One of the reaction partners was used in at least ten-fold excess over its counterpart. Under these pseudo-first order reaction conditions, the first-order rate constants k_{obs} (s^{-1}) were derived by least squares-fitting of the mono-exponential function

$$A_t = A_0 [1 - \exp(-k_{\text{obs}}t)] + C$$

to the time-dependent experimental absorbances A_t .

Only the reaction of the colored nucleophile **12d** with **11a** was followed by monitoring the consumption of **12d** during the reaction, as indicated by the decay of the **12d** absorption at $\lambda = 537$ nm. Pseudo-first order reaction conditions were established by using **11a** in an at least ten-fold excess over **12d**. First-order rate constants k_{obs} (s^{-1}) were derived by least squares-fitting of the mono-exponential decay function

$$A_t = A_0 \exp(-k_{\text{obs}}t) + C$$

to the time-dependent experimental absorbances A_t .

The second-order rate constants k_2 ($\text{M}^{-1} \text{s}^{-1}$) were then calculated as the slopes of the linear correlations of k_{obs} (s^{-1}) with four to five different concentrations of the excess reaction partner (Figure S2c). In several kinetic experiments, the crown ether 18-crown-6 was added, which partially complexes the K^+ counterions of the carbanions.^{5,5} Data points of kinetic measurements with and without added crown ether were treated indiscriminant and used jointly for the determination of k_2 .

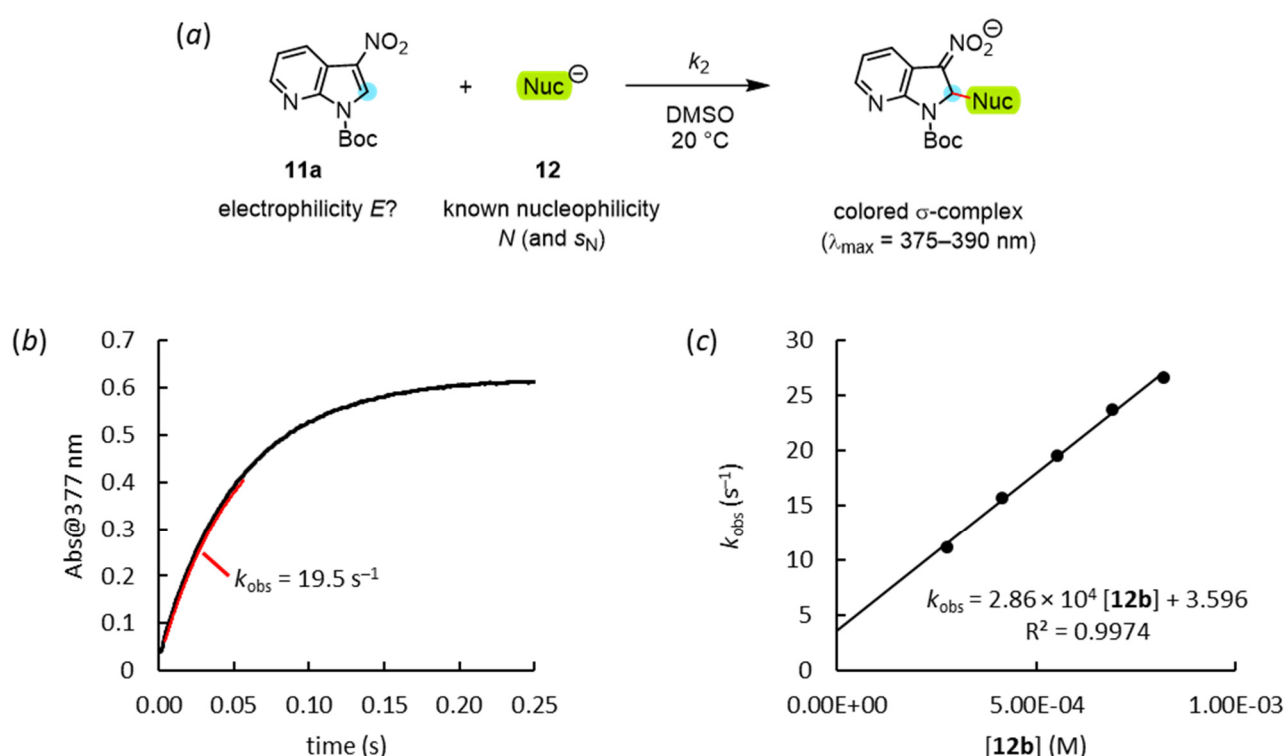
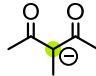
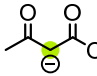
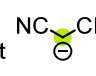
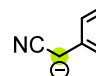
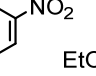
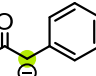
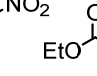


Figure S2: (A) The carbon-carbon bond-forming reaction of an carbanionic nucleophile with the electron-deficient arene **11a** gives a colored σ -complex. (B) Time-dependent increase of the absorbance in the reaction of **11a** ($c_0 = 2.74 \times 10^{-5} \text{ M}$) + **12b** ($c_0 = 5.52 \times 10^{-4} \text{ M}$) in DMSO at 20°C due to the formation of the colored σ -complex **11a+12b** as monitored at 377 nm. Curve fitting (red part of the curve) was used to determine the observed (pseudo-)first order rate constant k_{obs} (s^{-1}). (C) Linear correlation of experimentally determined first-order rate constants k_{obs} (s^{-1}) with the concentration of **12b** as required by the relationship $k_{\text{obs}} = k_2[\mathbf{12b}]$. The slope of the linear correlation corresponds to the second-order rate constant k_2 ($\text{M}^{-1} \text{s}^{-1}$).

The second-order rate constants of all kinetically investigated combinations of the electrophilic **11a** with the carbanionic reference nucleophiles **12a–12g** are listed in Table S1. Details of the individual kinetic measurements are given in Section 2.4.

Table S1. Summary of experimentally determined second-order rate constants k_2^{exp} for the reactions of **11a** with carbanions **12a–12g** (reference nucleophiles) in DMSO at 20 °C.

| $\text{:Nuc}^\ominus = $ <div style="display: flex; justify-content: space-around; align-items: center;"> <div style="text-align: center;">  12a </div> <div style="text-align: center;">  12b </div> <div style="text-align: center;">  12c </div> <div style="text-align: center;">  12d </div> <div style="text-align: center;">  12e </div> <div style="text-align: center;">  12f </div> <div style="text-align: center;">  12g </div> </div> | | | | | |
|---|--------------|--|------------------------|------------------------------|----------------|
| Nucleophiles | $N (s_N)$ | $k_2^{\text{exp}} (\text{M}^{-1} \text{s}^{-1})$ | $\lg k_2^{\text{exp}}$ | $(\lg k_2^{\text{exp}})/s_N$ | $\lg k_2^{S1}$ |
| 12a | 18.38 (0.72) | 1.06×10^4 | 4.03 | 5.59 | 3.99 |
| 12b | 18.82 (0.69) | 2.87×10^4 | 4.46 | 6.46 | 4.13 |
| 12c | 19.36 (0.67) | 2.81×10^4 | 4.45 | 6.64 | 4.37 |
| 12d | 19.67 (0.68) | 3.09×10^4 | 4.49 | 6.60 | 4.64 |
| 12e | 20.00 (0.71) | 7.58×10^4 | 4.88 | 6.87 | 5.08 |
| 12f | 20.22 (0.65) | 1.23×10^5 | 5.09 | 7.83 | 4.80 |
| 12g | 21.13 (0.68) | 1.88×10^5 | 5.27 | 7.76 | 5.64 |
| Electrophilicity E of 11a | | −12.84 | | | |

Rearranging the Mayr-Patz equation (S1)

$$\lg k_2(20^\circ\text{C}) = s_N(N + E) \quad (\text{S1})$$

to equation (S2)

$$(\lg k_2)/s_N = N + E \quad (\text{S2})$$

enables to depict the kinetic data of Table S1 as a linear correlation (Figure S3), which illustrates the results of the least-square minimization $\Delta^2 = (\lg k_2^{\text{exp}} - s_N(N + E))^2$ to calculate the electrophilicity parameter E of **11a**. The least-squares minimizations used the second-order rate constants k_2 in DMSO at 20 °C from Table S1 and the reported nucleophile-specific reactivity parameters N and s_N of the reference nucleophiles **12a–12g** as input in an MS Excel spreadsheet. The E parameter was defined as the only adjustable variable and optimized by using the MS Excel Solver (GRG algorithm).

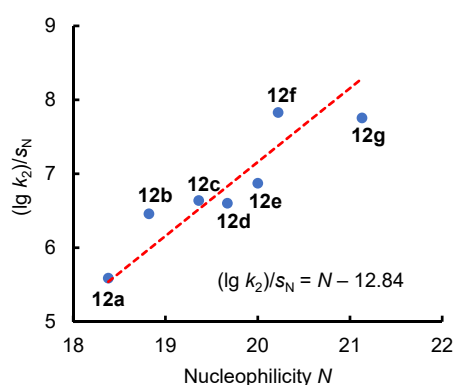


Figure S3: Plot of $(\lg k_2)/s_N$ vs. nucleophilicity N to illustrate the precision of the electrophilicity parameter $E = -12.84$ of **11a**, which was calculated by a least-squares minimization of $\Delta^2 = (\lg k_2 - s_N(N + E))^2$ with E as the only adjustable. The slope of the correlation line was enforced to unity as required by equation S1.

2.2 NMR and HRMS detection of covalent adducts of carbanions and **11a**

2.2.1 General procedure

In glove box, a solution of the 7-aza-3-nitro-indole **11a** (0.1 mmol, in 0.4 mL DMSO-*d*₆) and a solution of the nucleophile **12** (0.1 mmol, in 0.4 mL DMSO-*d*₆) were mixed at room temperature. Subsequently, the reaction mixture was analyzed by NMR spectroscopy and HRMS without further workup.

4.2.2 Wheland adduct **WA1** from the reaction of **11a** with **12a** (TZ1d5)

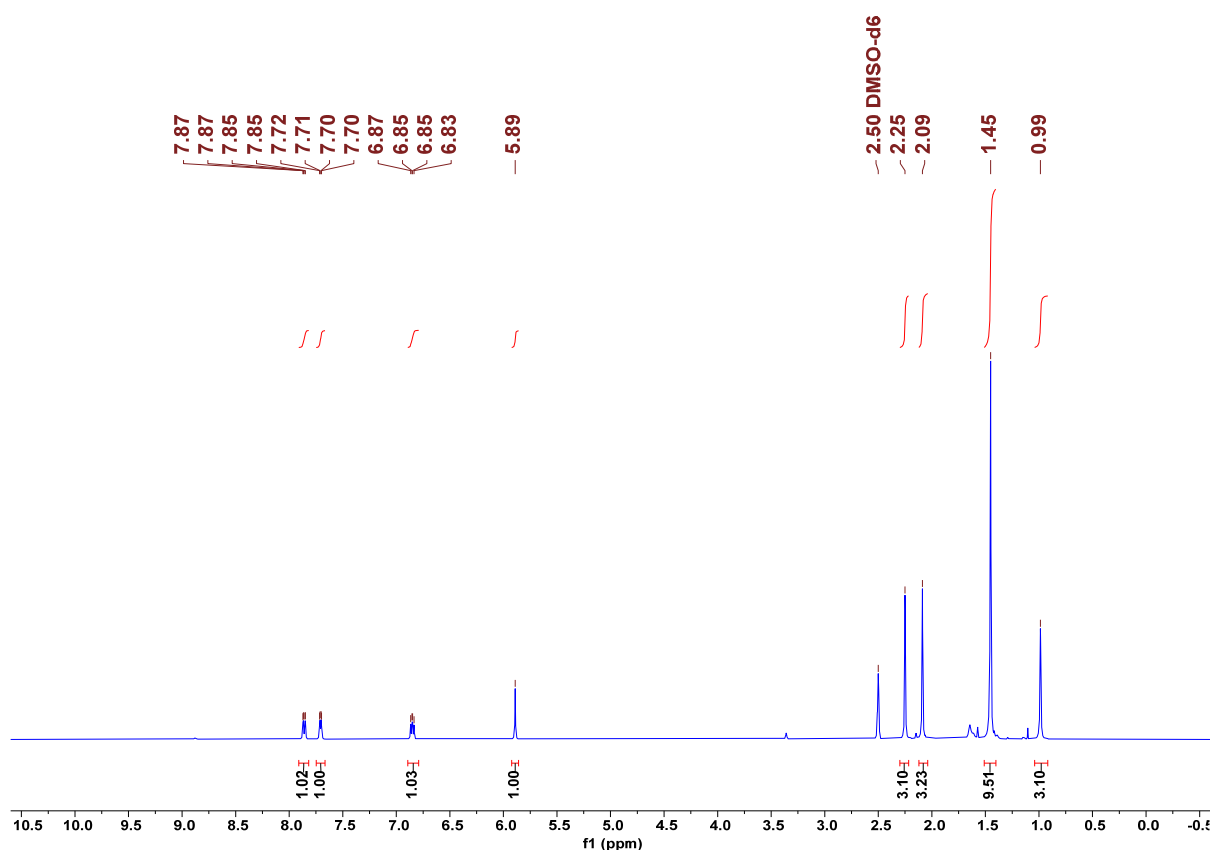
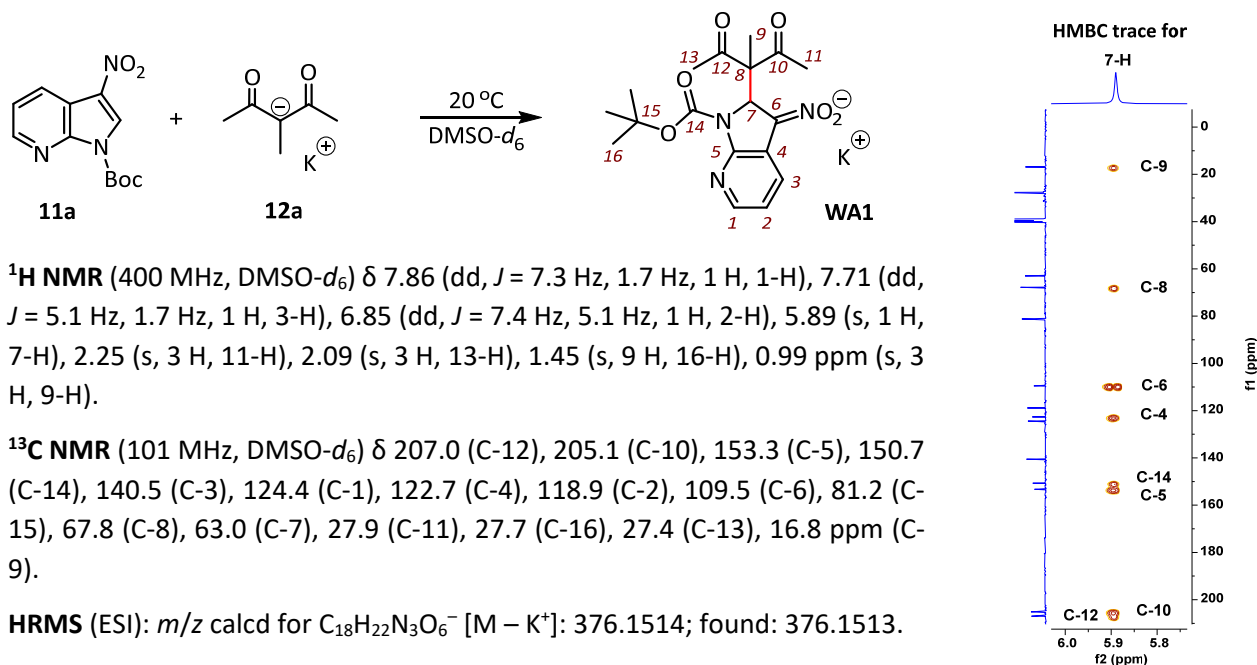


Figure S4: ¹H NMR spectrum (400 MHz) of the adduct **WA1** in DMSO-*d*₆.

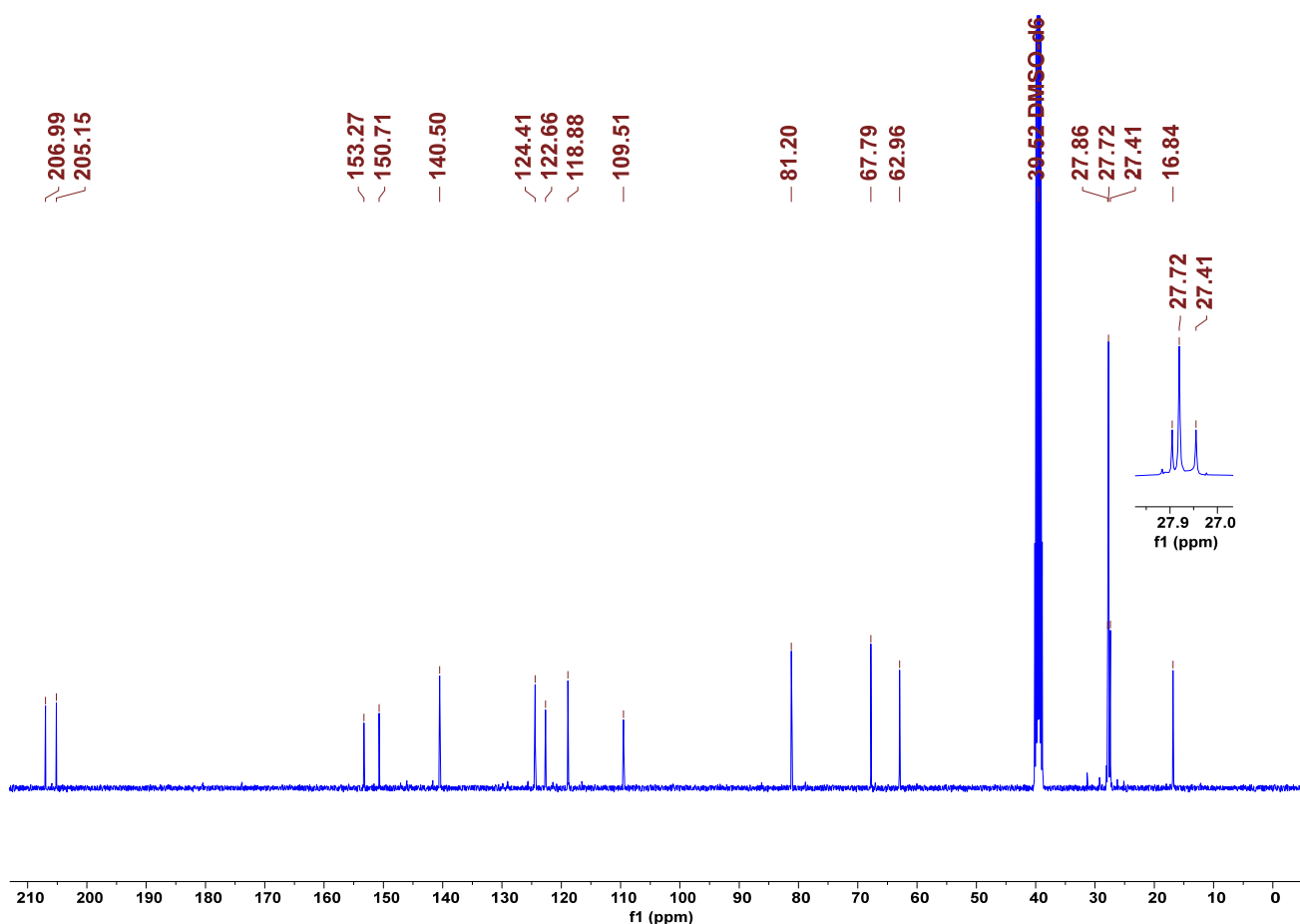
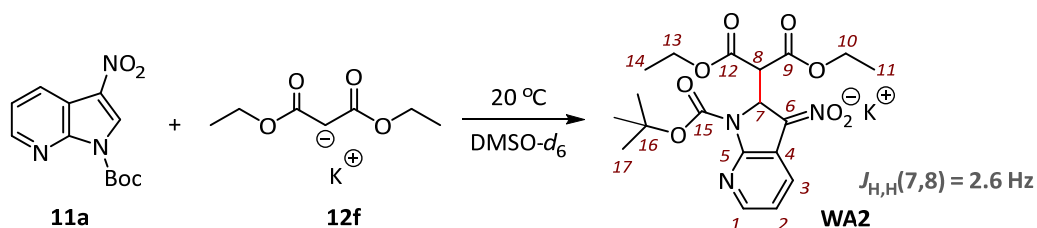


Figure S5: ^{13}C NMR spectrum (101 MHz) of the adduct **WA1** in $\text{DMSO-}d_6$.

4.2.3 Wheland adduct **WA2** from the reaction of **11a** with **12f** (TZ1d3)



^1H NMR (400 MHz, $\text{DMSO-}d_6$) δ 7.80 (dd, $J = 7.4$ Hz, 1.8 Hz, 1 H, 1-H), 7.65 (dd, $J = 5.1$ Hz, 1.8 Hz, 1 H, 3-H), 6.77 (dd, $J = 7.4$ Hz, 5.1 Hz, 1 H, 2-H), 5.59 (d, $J = 2.6$ Hz, 1 H, 7-H), 4.52 (d, $J = 2.6$ Hz, 1 H, 8-H), 4.08–4.02 (m, 2 H, 10-H), 3.90–3.83 (m, 2 H, 13-H), 1.46 (s, 9 H, 17-H), 1.13 (t, $J = 7.2$ Hz, 3 H, 11-H), 0.93 ppm (t, $J = 7.1$ Hz, 3 H, 14-H).

^{13}C NMR (101 MHz, $\text{DMSO-}d_6$) δ 167.1 (C_q , C-9), 166.4 (C_q , C-12), 153.6 (C_q , C-5), 150.7 (C_q , C-15), 140.3 (CH, C-3), 124.0 (CH, C-1), 122.5 (C_q , C-4), 118.2 (CH, C-2), 109.9 (C_q , C-6), 80.6 (C_q , C-16), 60.6 (CH_2 , C-10), 60.2 (CH_2 , C-13), 60.1 (CH, C-7), 50.8 (CH, C-8), 27.9 (CH_3 , C-17), 13.9 (CH_3 , C-11), 13.6 ppm (CH_3 , C-14).

HRMS (ESI): m/z calcd for $\text{C}_{19}\text{H}_{24}\text{N}_3\text{O}_8^-$ [$\text{M} - \text{K}^+$]: 422.1569; found: 422.1563.

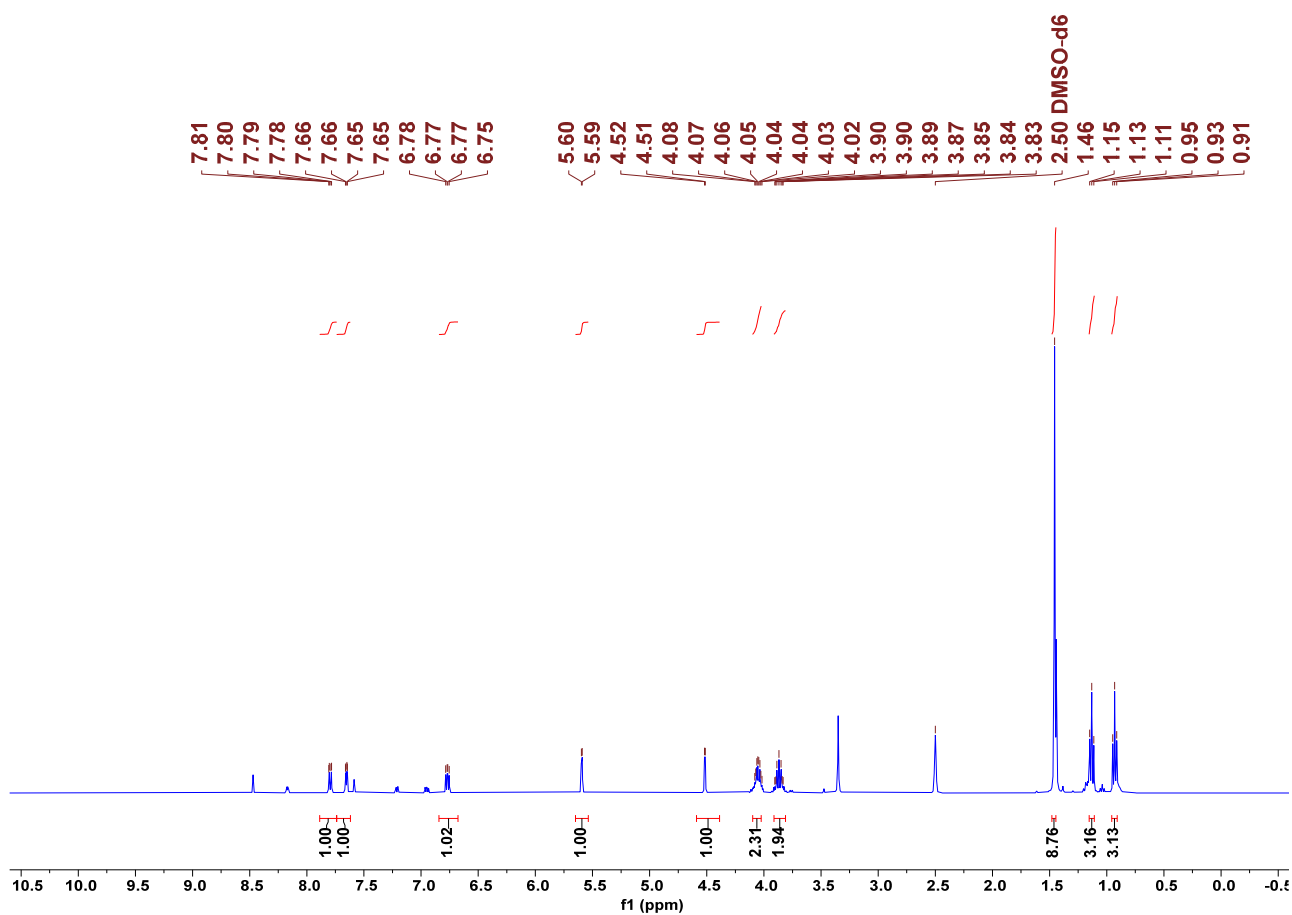


Figure S6: ¹H NMR spectrum (400 MHz) of the adduct **WA2** in DMSO-*d*₆.

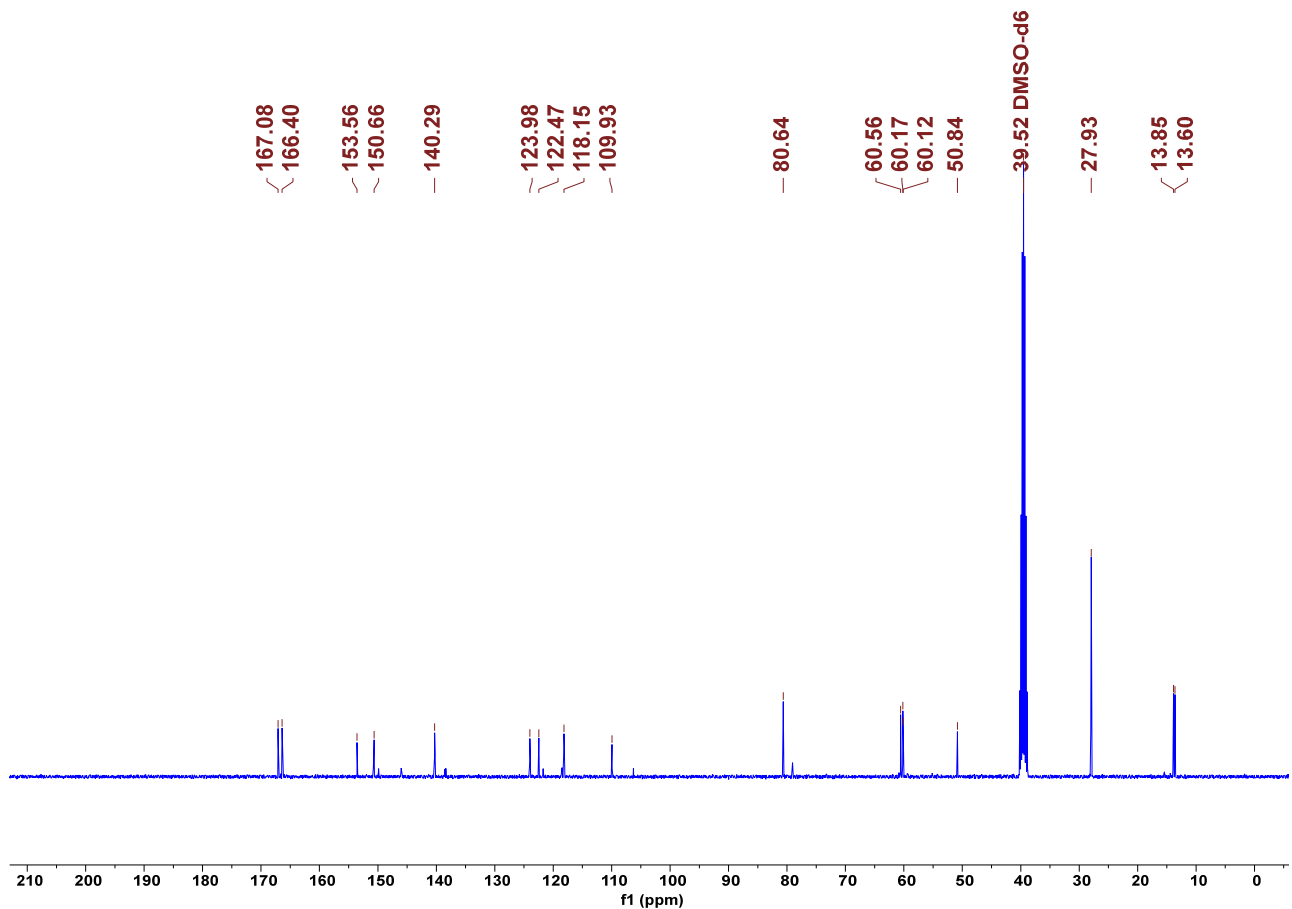
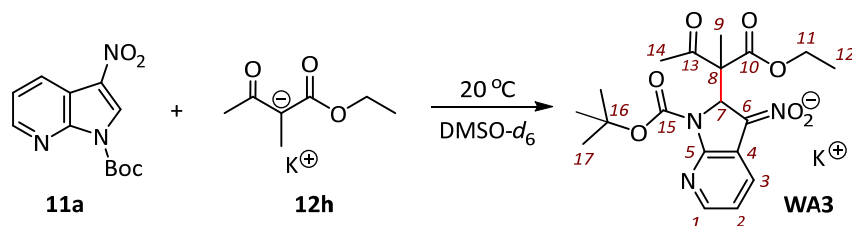


Figure S7: ¹³C NMR spectrum (101 MHz) of the adduct **WA2** in DMSO-*d*₆.

4.2.4 Wheland adduct **WA3** from the reaction of **11a** with **12h** (TZ1d7)



The adduct **WA3** was generated as a diastereomeric mixture (*dr* ~ 2:3). In the subsequent list of characterization data, * marks resonances of the major diastereomer.

¹H NMR (400 MHz, DMSO-*d*₆): δ = 7.86–7.83 (m, 1 H, both isomers, 1-H), 7.70–7.67 (m, 1 H, both isomers, 3-H), 6.84–6.80 (m, 1 H, both isomers, 2-H), 5.98*/5.89 (2 s, 1 H, 7-H), 4.01*/3.93 (2 q, each with *J* = 7.1 Hz, 2 H, 11-H), 2.38*/2.31 (2 s, 3 H, 14-H), 1.45*/1.44 (2 s, 9 H, 17-H), 1.15*/1.08 (2 t, each with *J* = 7.1 Hz, 3 H, 12-H), 1.00/0.95* ppm (2 s, 3 H, 9-H).

¹³C NMR (101 MHz, DMSO-*d*₆): δ = 204.2/202.2* (C_q, C-13), 171.3*/171.0 (C_q, C-10), 153.3*/153.2 (C_q, C-5), 150.82*/150.78 (C_q, C-15), 140.4*/140.0 (CH, C-3), 124.3*/124.2 (CH, C-1), 123.0/122.7* (C_q, C-4), 118.7/118.5* (CH, C-2), 109.6/109.3* (C_q, C-6), 81.0/80.7* (C_q, C-16), 63.3/62.9*/62.3* (C-7 and C-8), 60.55*/60.51 (CH₂, C-11), 28.0/27.9* (CH₃, C-14), 27.8/27.7* (CH₃, C-17), 17.5/16.8* (CH₃, C-9), 13.70/13.67* ppm (CH₃, C-12).

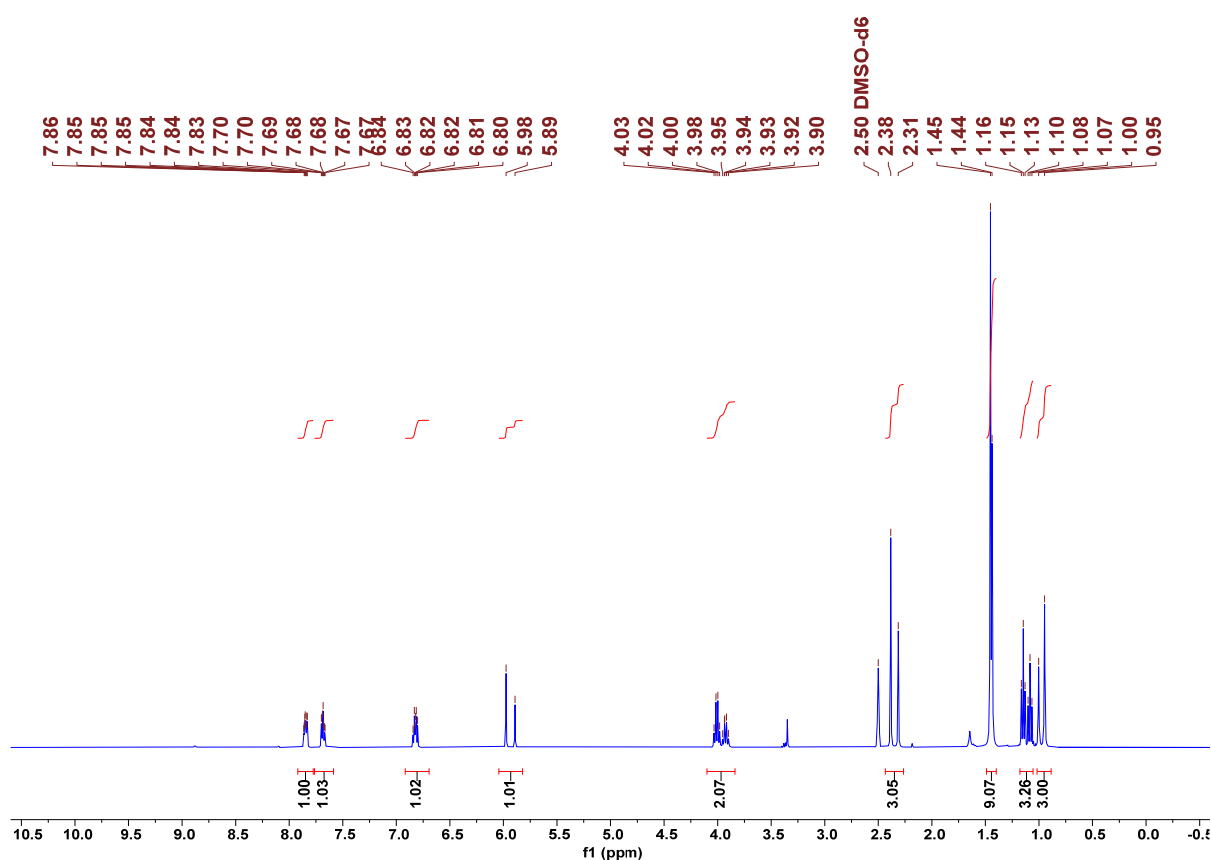
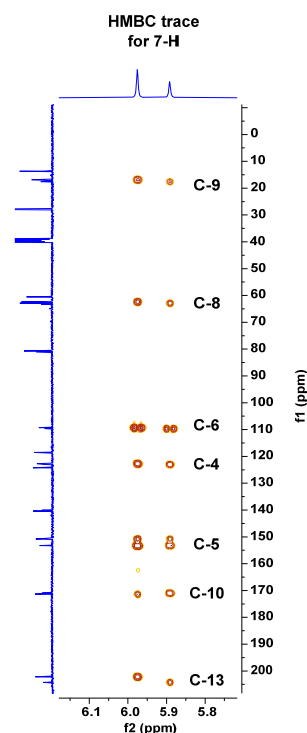


Figure S8: ¹H NMR spectrum (400 MHz) of the adducts **WA3** (*dr* ~ 2:3) in DMSO-*d*₆.

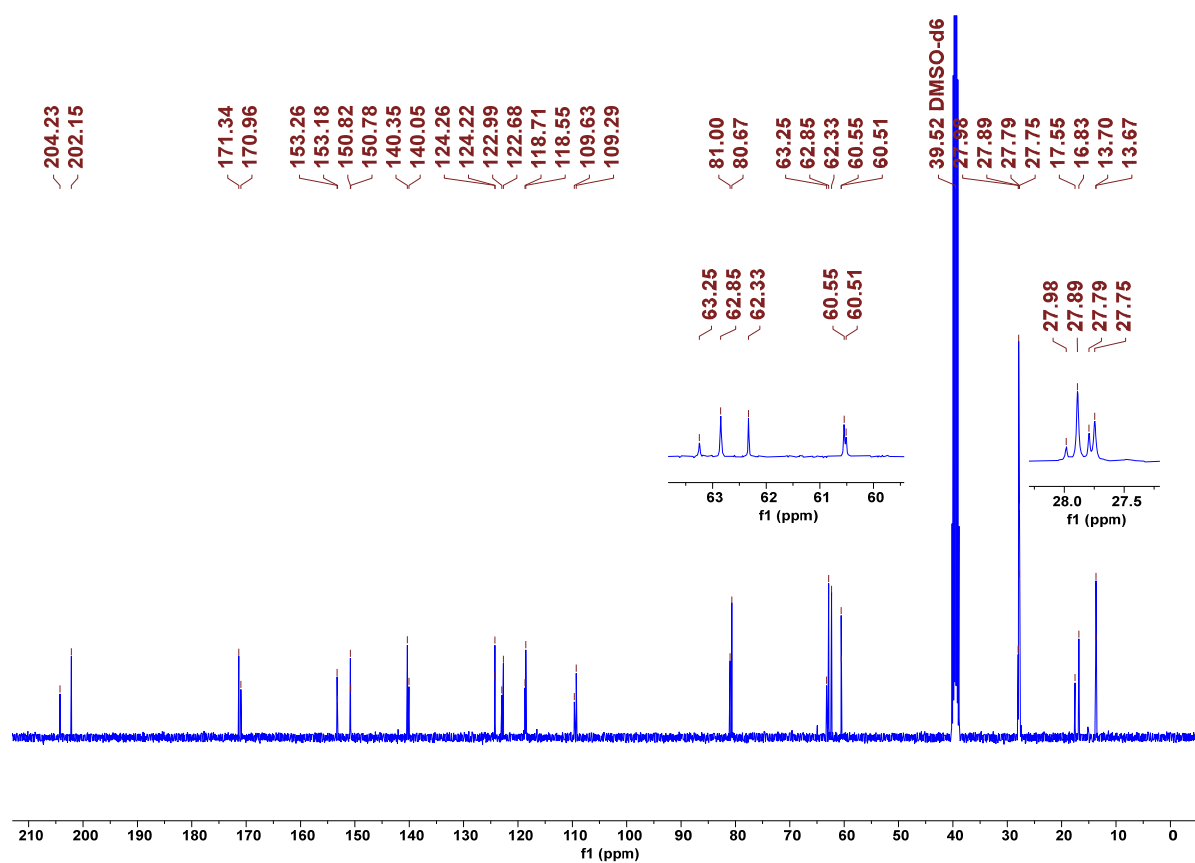


Figure S9: ^{13}C NMR spectrum (101 MHz) of the adducts **WA3** ($dr \sim 2:3$) in $\text{DMSO-}d_6$.

2.3 UV-Vis spectra of mixtures of C-nucleophiles (**12**) with the **11a**

After recording the UV-Vis spectrum of the pure indole **11a** in DMSO (Figure S9), further UV-Vis spectra were acquired for mixtures of **11a** with an excess of the reference nucleophiles **12a–12g** (Figures S10–S16) to identify a suitable wavelength for the online monitoring of the reaction kinetics.

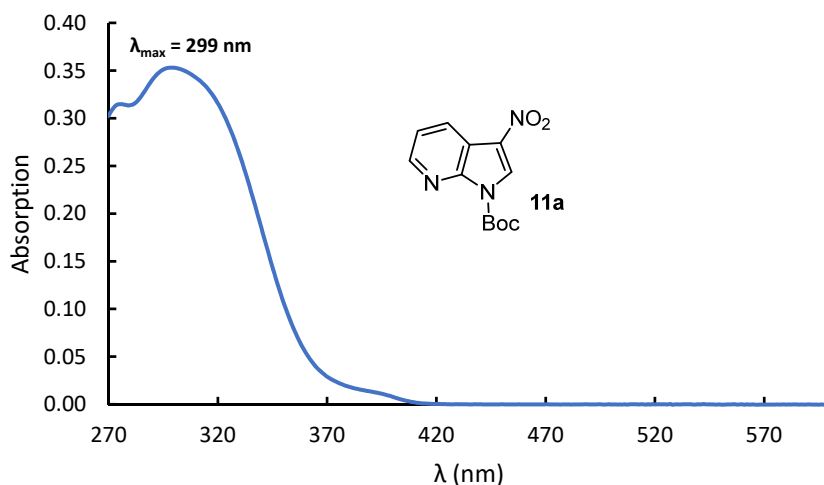


Figure S10: UV-Vis spectrum of **11a** in DMSO (recorded by using a diode array spectrometer).

For evaluating the changes in the UV-Vis spectra during the reactions of **11a** with **12a–12g**, a DMSO solution of the indole **11a** and a DMSO solution of nucleophile **12** were mixed in a flask filled with DMSO. The spectral changes of the reaction mixture were followed by utilizing a diode array photometer (J&M TIDAS).

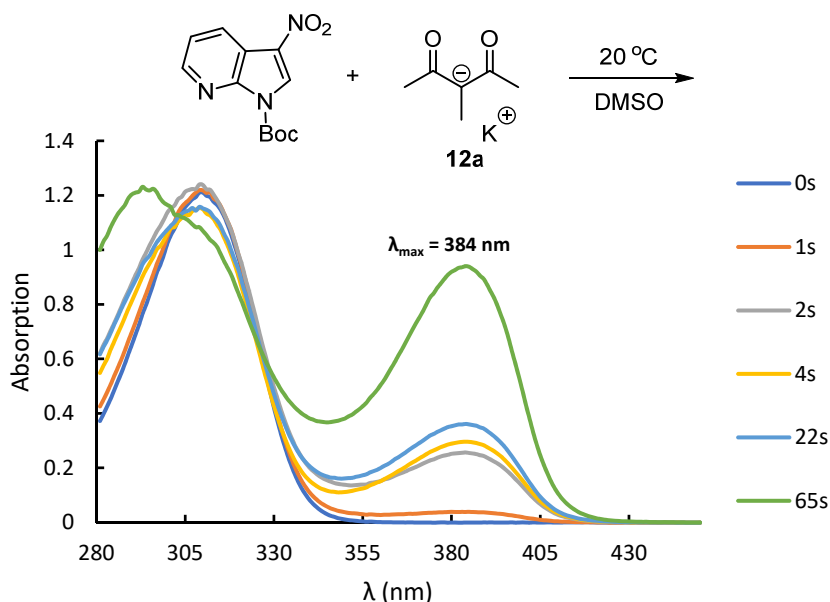
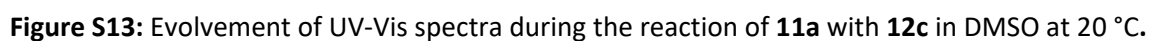
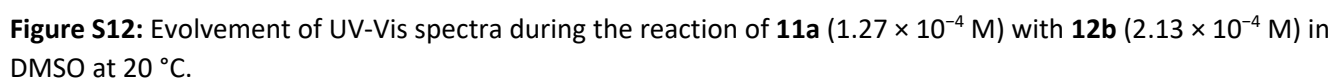
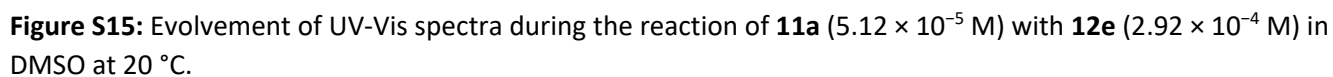
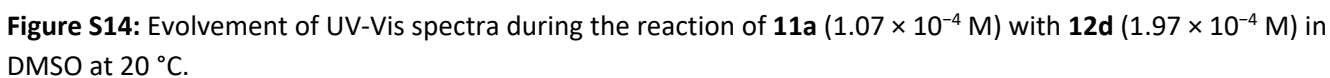


Figure S11: Evolution of UV-Vis spectra during the reaction of **11a** (1.27×10^{-4} M) with **12a** (2.35×10^{-4} M) in DMSO at 20 °C.





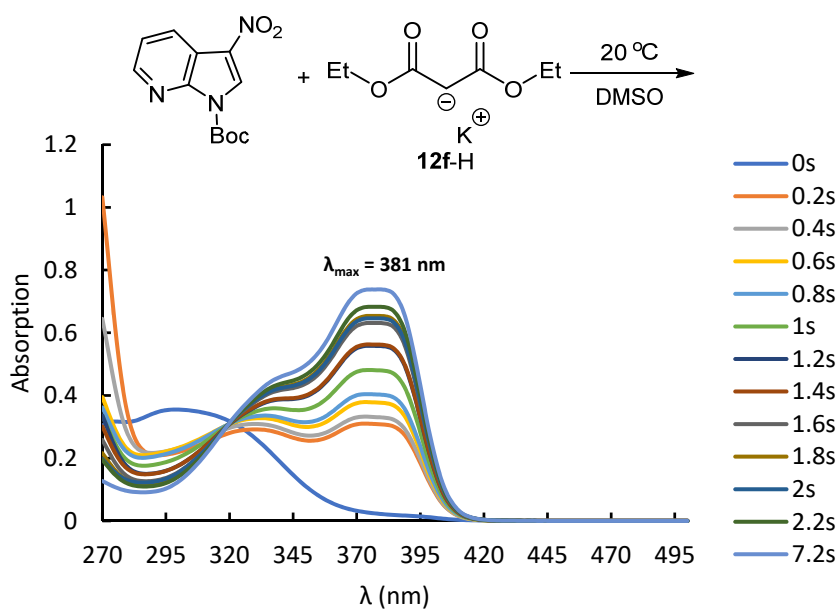


Figure S16: Evolution of UV-Vis spectra during the reaction of **11a** (1.05×10^{-4} M) with **12f** (1.13×10^{-4} M) in DMSO at 20 °C.

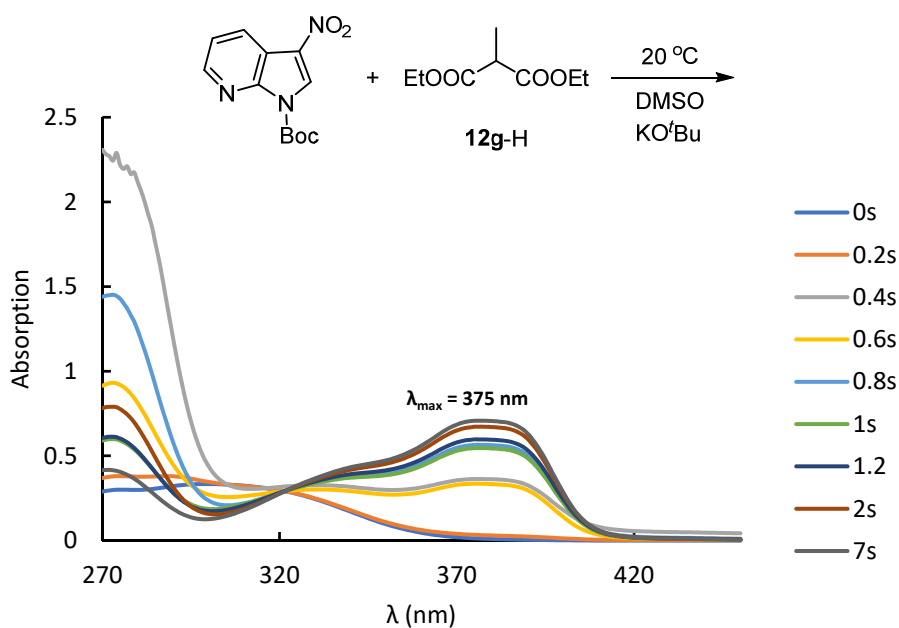
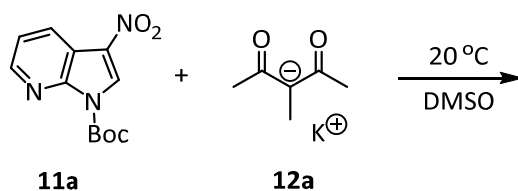


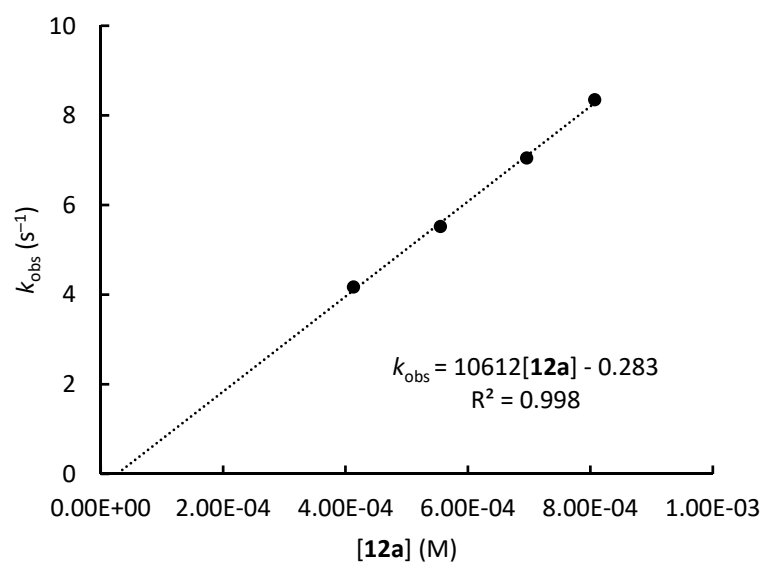
Figure S17: Evolution of UV-Vis spectra during the reaction of **11a** (1.08×10^{-5} M) with **12g** (1.63×10^{-5} M) in DMSO at 20 °C.

2.4 Kinetics of the reactions of **11a** with carbanions (reference nucleophiles **12**)

Table S2: Kinetics of the reaction of **11a** with preformed **12a** in DMSO at 20 °C (1:1 single mixing stopped-flow UV-Vis spectrometer, increase at 384 nm).

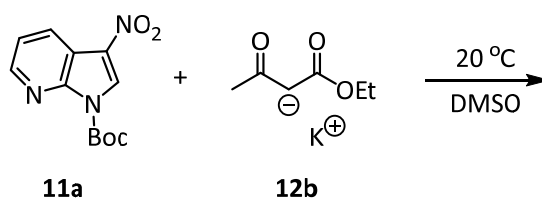


| [11a] (M) | [12a] (M) | [18-c-6] (M) | [12a]/[11a] | k_{obs} (s ⁻¹) |
|-----------------------|-----------------------|-----------------------|-------------------------------|-------------------------------------|
| 2.78×10^{-5} | 4.13×10^{-4} | 4.55×10^{-4} | 15 | 4.17 |
| 2.78×10^{-5} | 5.55×10^{-4} | | 20 | 5.52 |
| 2.78×10^{-5} | 6.96×10^{-4} | 7.66×10^{-4} | 25 | 7.05 |
| 2.78×10^{-5} | 8.07×10^{-4} | | 29 | 8.35 |

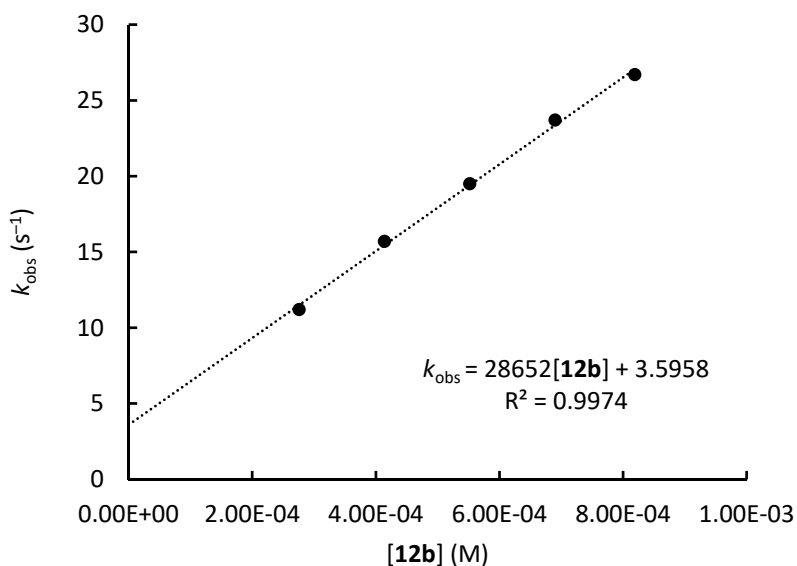


$$k_2 = (1.06 \pm 0.03) \times 10^4 \text{ M}^{-1} \text{ s}^{-1}$$

Table S3: Kinetics of the reaction of **11a** with preformed **12b** in DMSO at 20 °C (1:1 single mixing stopped-flow UV-Vis spectrometer, increase at 377 nm).

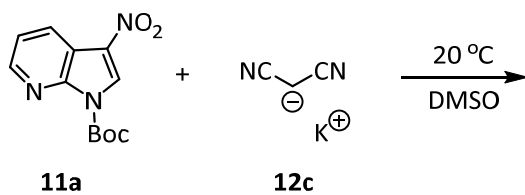


| [11a] (M) | [12b] (M) | [18-c-6] (M) | [12b]/[11a] | k_{obs} (s ⁻¹) |
|-----------------------|-----------------------|-----------------------|-------------------------------|-------------------------------------|
| 2.74×10^{-5} | 2.76×10^{-4} | | 10 | 1.12×10^1 |
| 2.74×10^{-5} | 4.14×10^{-4} | 4.55×10^{-4} | 15 | 1.57×10^1 |
| 2.74×10^{-5} | 5.52×10^{-4} | | 20 | 1.95×10^1 |
| 2.74×10^{-5} | 6.90×10^{-4} | 7.59×10^{-4} | 25 | 2.37×10^1 |
| 2.74×10^{-5} | 8.19×10^{-4} | | 30 | 2.67×10^1 |

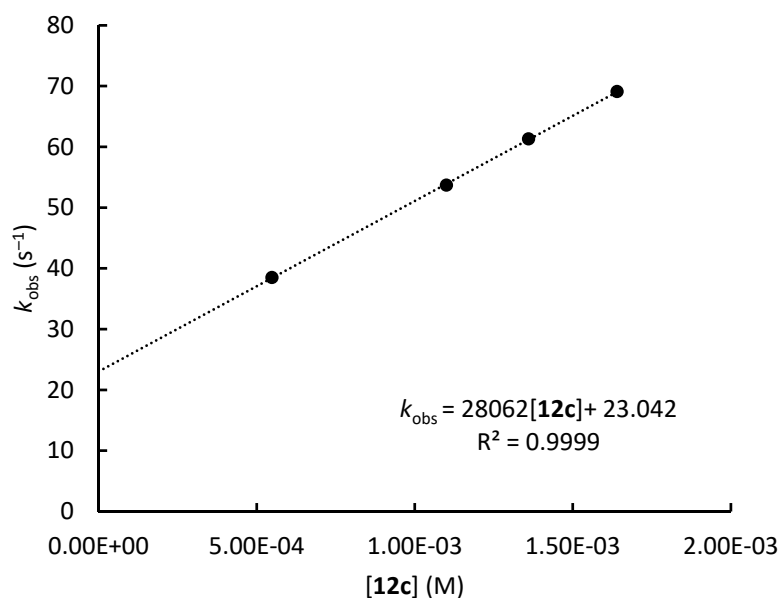


$$k_2 = (2.87 \pm 0.09) \times 10^4 \text{ M}^{-1} \text{ s}^{-1}$$

Table S4: Kinetics of the reaction of **11a** with preformed **12c** in DMSO at 20 °C (1:1 single mixing stopped-flow UV-Vis spectrometer, increase at 390 nm).

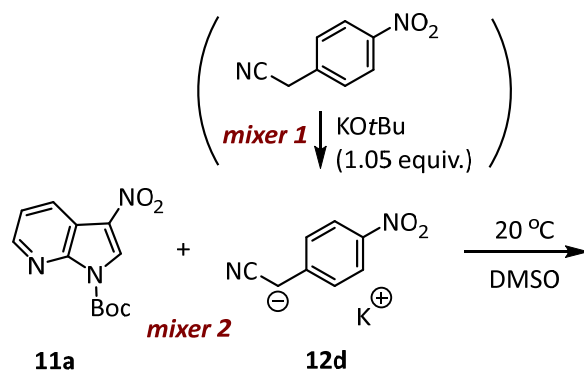


| [11a] (M) | [12c] (M) | [12c -H] (M) | [18-c-6] (M) | [12c]/[11a] | k_{obs} (s ⁻¹) |
|-----------------------|-----------------------|-----------------------|-----------------------|-------------------------------|-------------------------------------|
| 2.74×10^{-5} | 5.48×10^{-4} | 5.48×10^{-4} | | 20 | 3.85×10^1 |
| 2.74×10^{-5} | 1.10×10^{-3} | 1.10×10^{-3} | | 40 | 5.37×10^1 |
| 2.74×10^{-5} | 1.36×10^{-3} | 1.36×10^{-3} | 1.50×10^{-3} | 50 | 6.13×10^1 |
| 2.74×10^{-5} | 1.64×10^{-3} | 1.64×10^{-3} | | 60 | 6.91×10^1 |

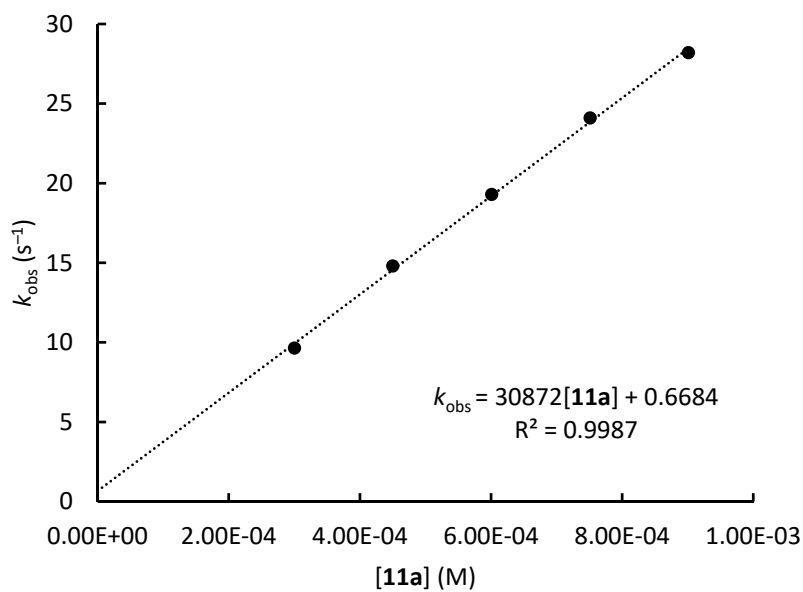


$$k_2 = (2.81 \pm 0.02) \times 10^4 \text{ M}^{-1} \text{ s}^{-1}$$

Table S5: Kinetics of the reaction of **11a** with **12d** in DMSO at 20 °C (sequential mixing stopped-flow UV-Vis spectrometer, decrease at 537 nm).

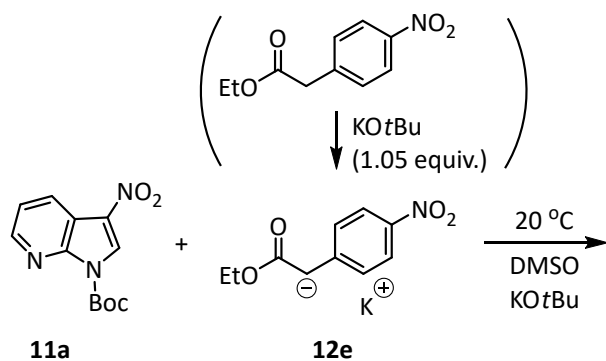


| [11a] (M) | [12d] (M) | [KOtBu] (M) | [11a]/[12d] | k_{obs} (s ⁻¹) |
|-----------------------|-----------------------|-----------------------|-------------------------------|-------------------------------------|
| 3.00×10^{-4} | 3.01×10^{-5} | 3.17×10^{-5} | 10 | 9.65 |
| 4.50×10^{-4} | 3.01×10^{-5} | 3.17×10^{-5} | 15 | 1.48×10^1 |
| 6.01×10^{-4} | 3.01×10^{-5} | 3.17×10^{-5} | 20 | 1.93×10^1 |
| 7.51×10^{-4} | 3.01×10^{-5} | 3.17×10^{-5} | 25 | 2.41×10^1 |
| 9.01×10^{-4} | 3.01×10^{-5} | 3.17×10^{-5} | 30 | 2.82×10^1 |

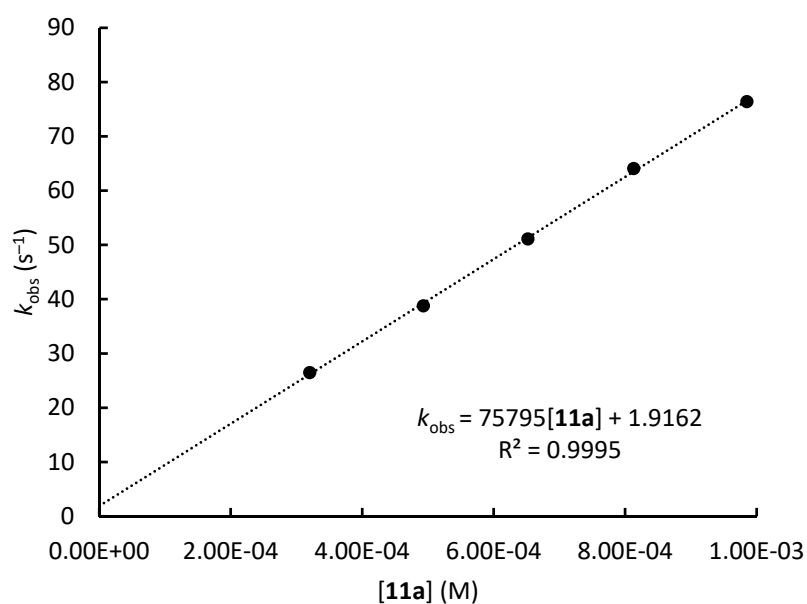


$$k_2 = (3.09 \pm 0.07) \times 10^4 \text{ M}^{-1} \text{ s}^{-1}$$

Table S6: Kinetics of the reaction of **11a** with **12e** in DMSO at 20 °C (**12e** was generated in DMSO solution from **12e-H** by addition of 1.05 equivalents of KO^tBu, 1:1 single mixing stopped-flow UV-Vis spectrometer, increase at 383 nm).

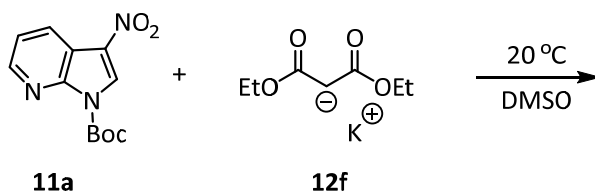


| [11a] (M) | [12e] (M) | [11a]/[12e] | k_{obs} (s ⁻¹) |
|-----------------------|-----------------------|-------------|-------------------------------------|
| 3.20×10^{-4} | 3.28×10^{-5} | 10 | 2.65×10^1 |
| 4.93×10^{-4} | 3.28×10^{-5} | 15 | 3.88×10^1 |
| 6.52×10^{-4} | 3.28×10^{-5} | 20 | 5.11×10^1 |
| 8.13×10^{-4} | 3.28×10^{-5} | 25 | 6.41×10^1 |
| 9.85×10^{-4} | 3.28×10^{-5} | 30 | 7.64×10^1 |

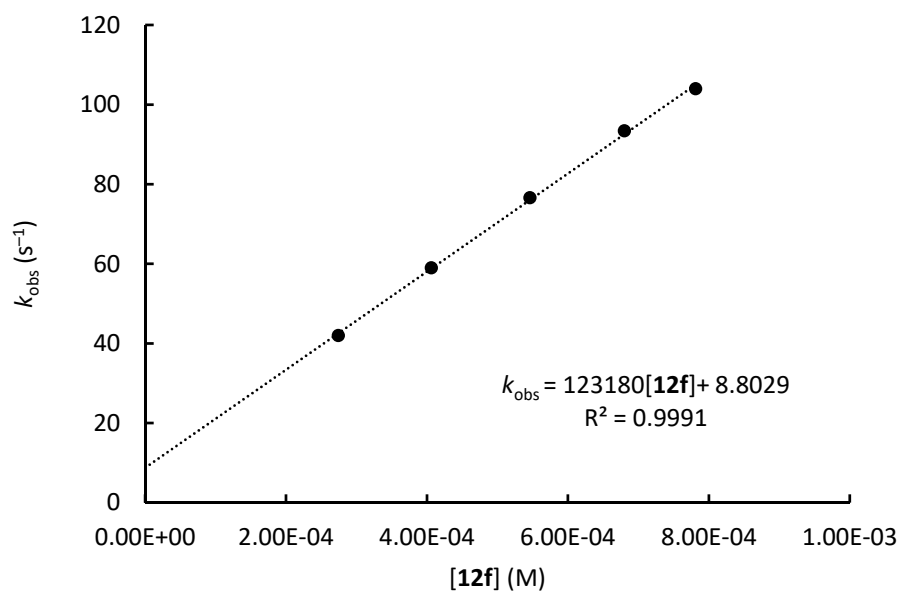


$$k_2 = (7.58 \pm 0.10) \times 10^4 \text{ M}^{-1} \text{ s}^{-1}$$

Table S7: Kinetics of the reaction of **11a** with preformed **12f** in DMSO at 20 °C (1:1 single mixing stopped-flow UV-Vis spectrometer, increase at 381 nm).

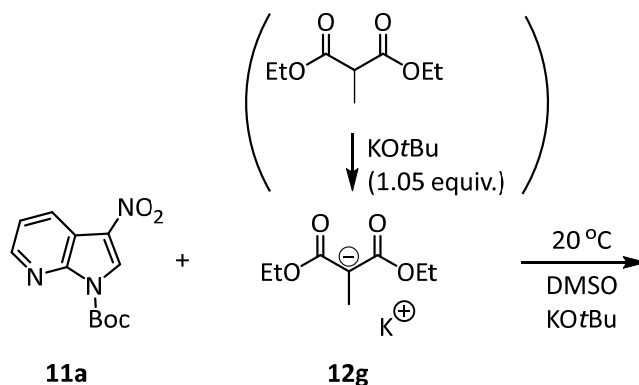


| [11a] (M) | [12f] (M) | [18-c-6] (M) | [12f]/[11a] | k_{obs} (s ⁻¹) |
|-----------------------|-----------------------|-----------------------|-------------------------------|-------------------------------------|
| 2.74×10^{-5} | 2.74×10^{-4} | | 10 | 4.20×10^1 |
| 2.74×10^{-5} | 4.06×10^{-4} | 4.47×10^{-4} | 15 | 5.90×10^1 |
| 2.74×10^{-5} | 5.46×10^{-4} | | 20 | 7.66×10^1 |
| 2.74×10^{-5} | 6.80×10^{-4} | 7.49×10^{-4} | 25 | 9.34×10^1 |
| 2.74×10^{-5} | 7.81×10^{-4} | | 29 | 1.04×10^2 |

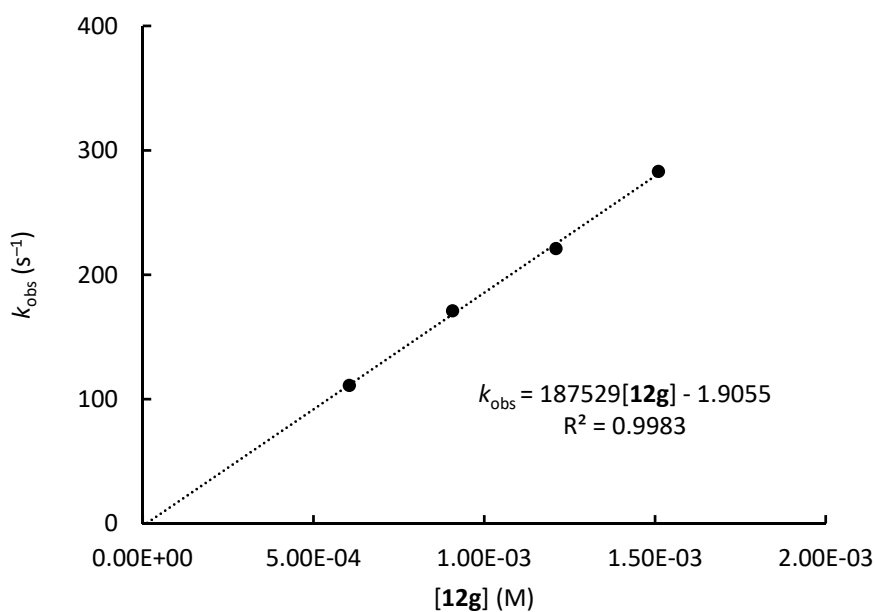


$$k_2 = (1.23 \pm 0.02) \times 10^5 \text{ M}^{-1} \text{ s}^{-1}$$

Table S8: Kinetics of the reaction of **11a** with **12g** in DMSO at 20 °C, (**12g** was generated in DMSO solution from **12g**-H by addition of 1.05 equivalents of KO^tBu, 1:1 single mixing stopped-flow UV-Vis spectrometer, increase at 375 nm).



| [11a] (M) | [12g] (M) | [18-c-6] (M) | [12g]/[11a] | k_{obs} (s ⁻¹) |
|-----------------------|-----------------------|-----------------------|-------------------------------|-------------------------------------|
| 6.02×10^{-5} | 6.05×10^{-4} | | 10 | 1.11×10^2 |
| 6.02×10^{-5} | 9.07×10^{-4} | 9.98×10^{-4} | 15 | 1.71×10^2 |
| 6.02×10^{-5} | 1.21×10^{-3} | | 20 | 2.21×10^2 |
| 6.02×10^{-5} | 1.51×10^{-3} | 1.66×10^{-3} | 25 | 2.83×10^2 |



$$k_2 = (1.88 \pm 0.06) \times 10^5 \text{ M}^{-1} \text{ s}^{-1}$$

3. References

-
- (S1) G. R. Fulmer, A. J. M. Miller, N. H. Sherden, H. E. Gottlieb, A. Nudelman, B. M. Stolz, J. E. Bercaw and K. I. Goldberg, *Organometallics*, 2010, **29**, 2176-2179.
- (S2) L. Birbaum, M. Ndiaye, M. Hachem, S. Perrio, M. De Paolis and I. Chataigner, *Org. Lett.*, 2025, **27**, 1729-1734.
- (S3) (a) R. Lucius, *Kinetische Untersuchungen zur Nucleophilie stabilisierter Carbanionen*, Dissertation, Ludwig-Maximilians-Universität München, 2001 (<https://doi.org/10.5282/edoc.257>). (b) M. Raban, E. A. Noe, G. Yamamoto, *J. Am. Chem. Soc.*, 1977, **99**, 6527-6531. (c) H. A. Dinçer, E. Gonca and A. Gül, *Dyes Pigm.*, 2008, **79**, 166-169. (d) Á. Puente, A. R. Ofial and H. Mayr, *Eur. J. Org. Chem.* 2017, **2017**, 1196-1202.
- (S4) The reactivity parameters N and s_N of the reference nucleophiles **12a–12g** were taken from the freely accessible database at <https://www.cup.uni-muenchen.de/oc/mayr/reaktionsdatenbank2/> (accessed on 06/05/2026); and refs. cited therein.
- (S5) V. P. Solov'ev, N. N. Strakhova, O. A. Raevsky, V. Rüdiger and H.-J. Schneider, *J. Org. Chem.*, 1996, **61**, 5221-5226.